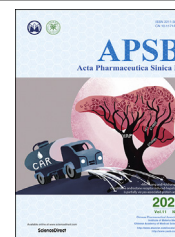




Chinese Pharmaceutical Association
Institute of Materia Medica, Chinese Academy of Medical Sciences

Acta Pharmaceutica Sinica B

www.elsevier.com/locate/apsb
www.sciencedirect.com



ORIGINAL ARTICLE

Isorhapontigenin protects against doxorubicin-induced cardiotoxicity *via* increasing YAP1 expression



Panxia Wang^a, Minghui Wang^a, Yuehuai Hu^a, Jianxing Chen^a,
Yanjun Cao^a, Cui Liu^a, Zhongkai Wu^e, Juan Shen^{d,*}, Jing Lu^{a,*},
Peiqing Liu^{a,b,c,*}

^aSchool of Pharmaceutical Sciences, Sun Yat-sen University, Guangzhou 510006, China

^bGuangdong Provincial Key Laboratory of New Drug Design and Evaluation, Sun Yat-sen University, Guangzhou 510006, China

^cGuangdong Provincial Engineering Laboratory of Druggability and New Drugs Evaluation, Guangzhou 510006, China

^dGuangdong Provincial Key Laboratory of Pharmaceutical Bioactive Substances, Guangdong Pharmaceutical University, Guangzhou 510006, China

^eDepartment of Cardiac Surgery, First Affiliated Hospital, Sun Yat-sen University, Guangzhou 510080, China

Received 21 June 2020; received in revised form 22 August 2020; accepted 24 August 2020

Abbreviations: AMPK, AMP-activated protein kinase; Ang II, angiotensin II; AP-1, anti-microbial protein; AREG, amphiregulin; AUC/Dose, dose-normalized plasma exposures; $C_{max}/Dose$, dose-normalized maximal plasma concentrations; CO, cardiac output; CTGF, connective tissue growth factor; DAB, 3,3'-diaminobenzidine; DMEM, Dulbecco's modified Eagle's medium; Dob, dobutamine; Dox, doxorubicin; EMT, epithelial mesenchymal transformation; FOXO1, forkhead box class O1; FS, fractional shortening; HE, hematoxylin–eosin; ISO, isoproterenol; Isor, isorhapontigenin; LVAW;d, left ventricular end-diastolic anterior wall thickness; LVAW;s, left ventricular end-systolic anterior wall thickness; LVID;d, left ventricular end-diastolic internal diameter; LVID;s, left ventricular end-systolic internal diameter; LVPW;d, left ventricular end-diastolic posterior wall thickness; LVPW;s, left ventricular end-systolic posterior wall thickness; LVEF, left ventricular ejection fraction; MAPK, mitogen-activated protein kinase; MI, myocardial infarction; NF- κ B, nuclear factor kappa-B; NRCMs, neonatal rat cardiomyocytes; P2Y12 receptor, ADP receptor; PGC-1 α , peroxisome proliferator-activated receptor γ coactivator-1 α ; PMSF, phenylmethanesulfonyl fluoride; PVDF, polyvinylidene fluoride; qRT-PCR, quantitative real-time polymerase chain reaction; ROS, reactive oxygen species; SD, Sprague–Dawley; SDS-PAGE, sodium dodecyl sulfate-polyacrylamide gel electrophoresis; sgRNAs, sequence guiding RNAs; SESN2, sestrin2; TCF4, T-cell factor 4; TEAD, TEA domain transcription factor proteins; TUNEL, TdT-mediated dUTP nick end labeling; WGA, wheat germ agglutinin; YAP1, Yes-associated protein 1; $\Delta\psi_m$, mitochondrial membrane potential.

*Corresponding authors.

E-mail addresses: liuq@mail.sysu.edu.cn (Peiqing Liu), lujing28@mail.sysu.edu.cn (Jing Lu), Shenjuan0412@126.com (Juan Shen).

Peer review under responsibility of Chinese Pharmaceutical Association and Institute of Materia Medica, Chinese Academy of Medical Sciences.

<https://doi.org/10.1016/j.apsb.2020.10.017>

2211-3835 © 2021 Chinese Pharmaceutical Association and Institute of Materia Medica, Chinese Academy of Medical Sciences. Production and hosting by Elsevier B.V. This is an open access article under the CC BY-NC-ND license (<http://creativecommons.org/licenses/by-nc-nd/4.0/>).

KEY WORDS

Isorhapontigenin;
YAP1;
Doxorubicin;
Cardiotoxicity;
Cardiomyocytes
apoptosis;
TEAD1;
Connective tissue growth
factor;
Amphiregulin

Abstract As an effective anticancer drug, the clinical limitation of doxorubicin (Dox) is the time- and dose-dependent cardiotoxicity. Yes-associated protein 1 (YAP1) interacts with transcription factor TEA domain 1 (TEAD1) and plays an important role in cell proliferation and survival. However, the role of YAP1 in Dox-induced cardiomyopathy has not been reported. In this study, the expression of YAP1 was reduced in clinical human failing hearts with dilated cardiomyopathy and Dox-induced *in vivo* and *in vitro* cardiotoxic model. Ectopic expression of *Yap1* significantly blocked Dox-induced cardiomyocytes apoptosis in TEAD1 dependent manner. Isorhapontigenin (Isor) is a new derivative of stilbene and responsible for a wide range of biological processes. Here, we found that Isor effectively relieved Dox-induced cardiomyocytes apoptosis in a dose-dependent manner *in vitro*. Administration with Isor (30 mg/kg/day, intraperitoneally, 3 weeks) significantly protected against Dox-induced cardiotoxicity in mice. Interestingly, Isor increased Dox-caused repression in YAP1 and the expression of its target genes *in vivo* and *in vitro*. Knockout or inhibition of *Yap1* blocked the protective effects of Isor on Dox-induced cardiotoxicity. In conclusion, YAP1 may be a novel target for Dox-induced cardiotoxicity and Isor might be a new compound to fight against Dox-induced cardiotoxicity by increasing YAP1 expression.

© 2021 Chinese Pharmaceutical Association and Institute of Materia Medica, Chinese Academy of Medical Sciences. Production and hosting by Elsevier B.V. This is an open access article under the CC BY-NC-ND license (<http://creativecommons.org/licenses/by-nc-nd/4.0/>).

1. Introduction

Doxorubicin (Dox) belongs to anthracyclines, one of the most frequently used chemotherapeutics for a wide range of malignancies, such as breast cancer and haematologic cancer¹. However, the clinical application of Dox is limited by its lethal cardiomyopathy, which is characterized by decrease in left ventricular ejection fraction (LVEF) or even heart failure^{1–4}. Dox induces irreversible cardiomyocytes apoptosis, reactive oxygen species (ROS) production, impaired respiration and mitochondrial dysfunction in a time- and dose-dependent manner^{2,5–12}. We previously reported that α -enolase and sestrin2 (SESN2) protects against Dox-induced cardiomyopathy by maintaining mitochondrial function or regulating mitophagy^{2,8}. Several ROS scavenger agents are identified to relieve Dox-induced cardiomyopathy, but the clinical results are not satisfied^{10,13,14}. Therefore, it is urgent to find new strategies to fight against Dox-induced cardiomyopathy.

Yes-associated protein (YAP1), a transcriptional coactivator and the terminal effector of Hippo pathway, is an important regulator of cell proliferation and survival^{15–18}. YAP1 notably co-activates with TEA domain transcription factor proteins (TEADs), thereby activating expression of cell cycle regulators and other target genes such as connective tissue growth factor (*CTGF*) and amphiregulin (*AREG*), to increase cell proliferation and reduce apoptosis^{17–20}. In mammal, YAP1 plays a pivotal role in the heart development, myocardial infarction (MI), and fibrosis^{18,19,21–24}. The deletion of *Yap1* in the embryonic hearts inhibits cardiomyocyte proliferation and results in prenatal lethality^{18,19}. In chronic MI, cardiomyocyte-specific deletion of *Yap1* exacerbates MI-induced cardiomyocyte apoptosis and cardiac dysfunction^{22,23}. However, the role of YAP1 and its pharmacological intervention in Dox-induced cardiomyopathy have not been reported.

Isorhapontigenin (Isor, 4,3',5'-trihydroxy-3-methoxystilbene), derived from Chinese herbs and grapes, is a new derivative of stilbene, and its chemical structure is similar to that of resveratrol^{25–29}. Isor has been reported to be responsible for a wide range of biological processes, including antioxidant²⁷, anti-

inflammation^{28,30}, anti-platelet activation²⁹, anti-leukemic³¹, anti-tumorigenic activities^{32–35} and cardioprotection^{27,36}. Isor could protect against cardiac hypertrophy by decreasing ROS and blocking mitogen-activated protein kinase (MAPK)/nuclear factor kappa-B (NF- κ B) signaling pathways^{27,36}. To date, cardioprotective effects of Isor on Dox-induced cardiomyopathy and its underlying mechanisms have also not been evaluated.

In this study, we found that the expression of YAP1 was reduced in clinical human failing hearts with dilated cardiomyopathy and Dox-induced cardiotoxicity *in vivo* and *in vitro*. Overexpression of *Yap1* protected cardiomyocytes against Dox-induced injury in a TEAD1-dependent manner. YAP1 may be a novel target for Dox-induced cardiotoxicity. Besides, Isor effectively increased Dox-inhibited YAP1 levels and reduced cardiomyocyte apoptosis, cardiac injury and heart dysfunction *in vivo* and *in vitro*. Knockout or inhibition of *Yap1* blocked the protective effects of Isor against Dox-induced cardiotoxicity. Isor might be a new candidate to fight against Dox-induced cardiotoxicity by increasing YAP1 expression.

2. Materials and methods**2.1. Human samples**

Human heart samples were obtained from patients undergoing heart transplantation because of end-stage heart failure with dilated cardiomyopathy ($n = 7$). Human heart samples without any heart disease ($n = 4$) were obtained from age-matched donors. The human heart samples were obtained from the Second Department of Cardiac Surgery, First Affiliated Hospital of Sun Yat-sen University (Guangzhou, China) and the ethic approval number was No. [2017]157. The study conformed to the principles outlined in the Declaration of Helsinki. Informed consent was obtained from the families of the subjects. Total mRNA was extracted from these samples and assayed by RNA sequencing analysis and quantitative real-time polymerase chain reaction (qRT-PCR).

2.2. Animal model of Dox-induced cardiotoxicity

C57BL/6 mice (male, weighing 20–30 g, SPF grade, Certification No. 44007200068106) were from the Experimental Animal Center of Sun Yat-sen University, Guangzhou, China. The animal experiments were approved by the Research Ethics Committee of Sun Yat-sen University (No. SYSU-IACUC-2019-000006) and were performed following the Guide for the Care and Use of Laboratory Animals (NIH Publication No. 85-23, revised 1996). Mice were randomly divided into the following groups: control group, Dox group and combined Isor with Dox group. Mice were intraperitoneally administrated with Dox by three equal dosages over a period of 2 weeks (the cumulative doses of Dox were 24 mg/kg)³⁵. Isor (30 mg/kg/day, CSN12333, CSNpharm, Chicago, IL, USA) was dissolved in 0.3 mol/L 2-hydroxypropyl β -cyclodextrin (Wacker, Burghausen, Germany) and intraperitoneally administrated to the mice one week before Dox stimulation^{26,28}. Mice in control group got the same volume of vehicle solvent in the same way.

2.3. Echocardiographic study

Two weeks later with Dox stimulation, echocardiography was performed to evaluate the left ventricular function. Two-dimensionally guided M-mode echocardiography was conducted with a Technos MPX ultrasound system (ESAOTE, Italy) according to our previous report³⁵. Basic cardiac function parameters were measured, such as ejection fraction (EF), fractional shortening (FS), left ventricular end-diastolic anterior wall thickness (LVAW;d), left ventricular end-systolic anterior wall thickness (LVAW;s), left ventricular end-diastolic posterior wall thickness (LVPW;d), left ventricular end-systolic posterior wall thickness (LVPW;s), left ventricular end-diastolic internal diameter (LVID;d), left ventricular end-systolic internal diameter (LVID;s) and cardiac output (CO).

After echocardiography, mice were anesthetized and sacrificed. Hearts were rapidly removed at diastole stage (with 0.1 mol/L KCl injection) and washed in ice-cold PBS for three times. And then, hearts were transected and the upper parts were fixed with 4% paraformaldehyde and embedded in paraffin. Histological cross sections (5–6 μ m thickness) of the hearts were stained with hematoxylin–eosin (HE) and wheat germ agglutinin (WGA) staining for morphometric measurement. DNA fragmentation of apoptotic cells was detected by TdT-mediated dUTP nick end labeling (TUNEL) staining (Service-bio, Wuhan, China). The expression of YAP1 in the heart of mice was detected by immunohistochemistry using YAP1 primary antibody, HRP-conjugated secondary antibody and 3,3'-diaminobenzidine (DAB) substrate. All slides were photographed by using EVOS FL Auto and five different images were quantified and were analyzed using ImageJ software.

2.4. Primary culture of neonatal rat cardiomyocytes

After anesthetized, 1- to 3-day-old Sprague–Dawley (SD) rats were sacrificed. Hearts of rats were removed immediately and washed three times in ice-cold sterile PBS. For cell suspensions collection, ventricles were minced and dispersed at 37 °C in 15–20 mL 0.08% trypsin solution approximately 12–14 times for 5–3.5 min each time. Cardiomyocytes were harvested by centrifugation for 5 min at 1800 \times g and re-suspended in Dulbecco's modified Eagle's medium (DMEM, Gibco, Life technologies

corporation, Grand Island, NY, USA) with 10% fetal bovine serum (FBS, Invitrogen, Carlsbad, CA, USA). For the differential attachment between cardiomyocyte and myocardial fibroblast, the suspensions were cultured in two flasks for 1 h at 37 °C with 5% CO₂ atmosphere. Finally, NRCMs were collected and seeded onto culture dishes with 5-bromodeoxyuridine (0.1 mmol/L, Thermo Fisher Scientific Inc., Waltham, MA, USA). Twelve hours later, cardiomyocytes were washed with PBS and culture medium was changed to fresh DMEM supplemented with 10% FBS. Dox (1 μ mol/L) was used to induce *in vitro* cardiotoxic responses.

2.5. RNA sequencing analysis

Total RNA was extracted from failing heart of human with dilated cardiomyopathy or NRCMs with Dox stimulation. RNA sequencing (RNAseq) analysis was performed by BGI (Beijing Genomics Institute, Shenzhen, China). In brief, mRNA with polyA tail was enriched with magnetic beads with OligodT. cDNA was synthesized in a high temperature system and purified by kit followed by RNAseq using the BGISEQ platform. Raw reads were filtered by using SOAPnuke software to generate clean reads. And then we compared clean reads to the reference genome sequence using HISAT (Hierarchical Indexing for Spliced Alignment of Transcripts) and Bowtie2. RSEM was used to calculate the gene expression level of each sample. Transcripts were assembled, differential expression analysis was performed and heatmap was made.

2.6. CRISPR/Cas9 sgRNA design, lentivirus production and infection

Sequence guiding RNAs (sgRNAs) were designed using the Zhang's laboratory website (<http://crispr.mit.edu/>). Oligo to the sgRNAs was synthesized and cloned into lenti-CRISPR v2 vectors (Addgene, plasmid#52961, Cambridge, MA, USA). The sequence of sgRNA targeting *Yap1* was as follows: gRNA: ACGACCTGGTGACCCGCCGG. Lentivirus was generated by co-transfected Lenti-CRISPR v2-gRNA construction, psPAX2 and pMD2.G into HEK293T cell line. Viral supernatants were harvested 48 h later. One milliliter of virus was added to the NRCMs plated in 6-well plates with 60%–70% confluence. After incubation for 4–6 h, culture medium was changed to fresh DMEM supplemented with 10% FBS and cultured for another 72 h. The knockout efficiency of *Yap1* was detected by Western blot.

2.7. Recombinant adenovirus infection and RNA interference

Recombinant adenovirus vector harboring *Yap1* cDNA was purchased from Hanbio Technology (Shanghai, China). The adenoviruses were amplified in HEK293A cell line and purified with a virus purification kit (Biomiga, San Diego, CA, USA). To over-express *Yap1*, cardiomyocytes were infected with adenovirus at the concentration of 2⁶ PFU for 48 h. Small interfering RNA (siRNA) targeting *Tead1* and negative control (NC) siRNA were obtained from GenePharma (Shanghai, China) and the sequences were si-*Tead1*-1: GCGGACTTAACTGCAATA, si-*Tead1*-2: TGGGAAACAAGTAGTAGAA, si-*Tead1*-3: CAGACTCGTACAACAAACA. RNA interference transfection was conducted by using Lipofectamine 2000 reagent (Invitrogen, Carlsbad, CA, USA) according to the manufacturer's instruction. qRT-PCR was conducted to determine the silencing efficiency.

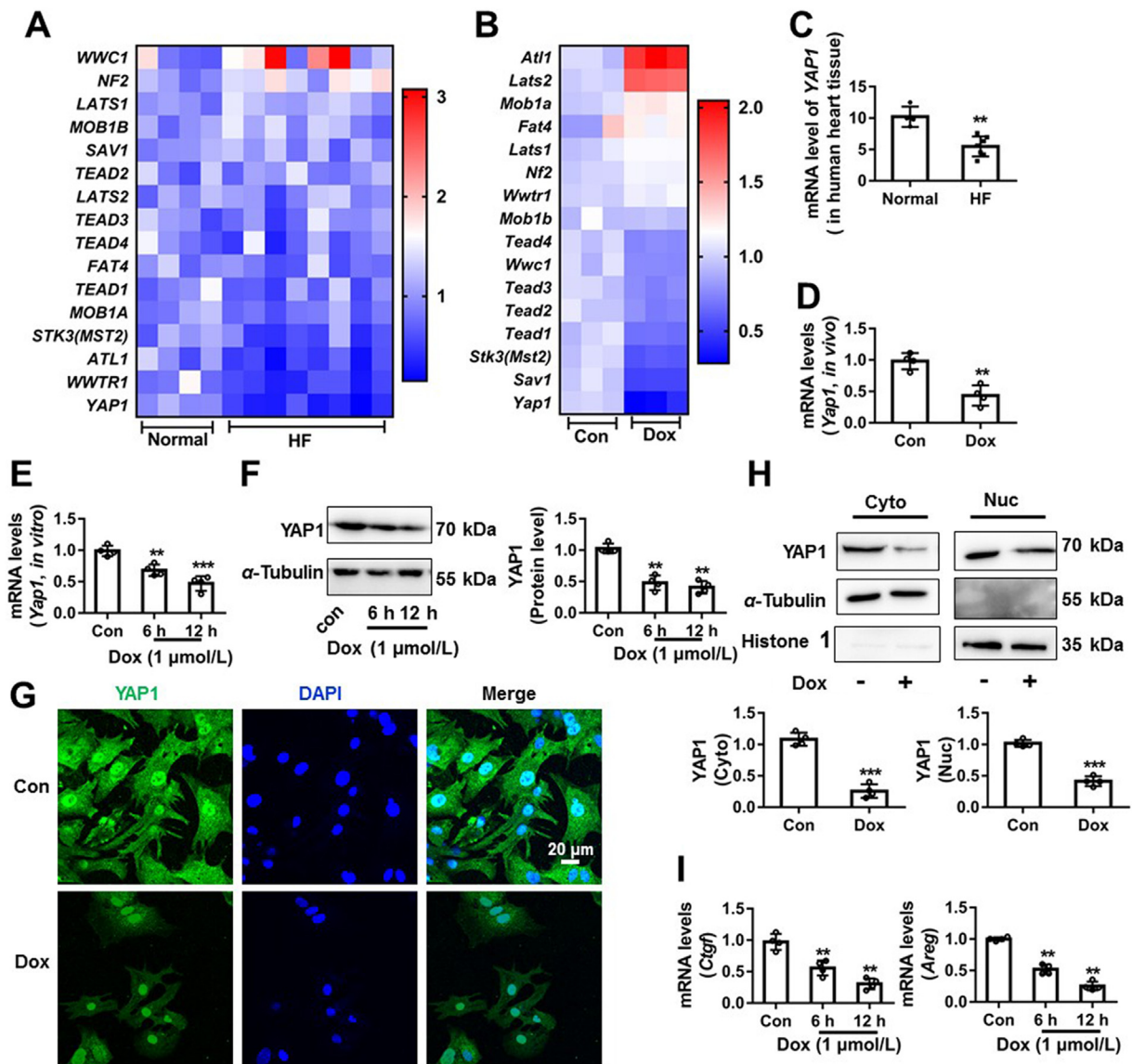


Figure 1 YAP1 expression was decreased in human failing hearts and in Dox-induced rat cardiotoxicity model. The expression changes of genes related to Hippo pathway in the human hearts with dilated cardiomyopathy (A) and in Dox-stimulated NRCMs were exhibited by heatmap (B). The change of *YAP1* mRNA expression in the human failing heart tissue was confirmed by qRT-PCR (C), $n = 4$ in control group and $n = 7$ in heart failure group. The change of *Yap1* mRNA expression in Dox-induced rat cardiotoxicity model was confirmed by qRT-PCR (D). NRCMs were treated with Dox (1 $\mu\text{mol/L}$) at different time point (0, 6 and 12 h). The mRNA expression of *Yap1* in NRCMs was measured by qRT-PCR (E). The protein expression of YAP1 in NRCMs was measured by Western blot (F) and IF assay (G, scale bar was 20 μm). The subcellular protein changes of YAP1 were measured by Western blot (H). The target genes changes of YAP1 were measured by qRT-PCR (I). Data were expressed as mean \pm SEM, $n = 4$; ** $P < 0.01$, *** $P < 0.001$ vs. control group. Dox, doxorubicin; NRCMs, neonatal rat cardiomyocytes; qRT-PCR, quantitative real-time polymerase chain reaction; YAP1, Yes-associated protein 1; IF, immunofluorescence.

Additional materials and methods were attached in the Supporting Information.

2.8. Statistical analysis

Data are expressed as mean \pm standard error of mean (SEM). Statistical analyses of two groups were performed using Student's *t*-tests. One-way ANOVA with Dunnett *post hoc* multiple comparisons were used for multiple comparisons (GraphPad Prism 6.0 software, San Diego, CA, USA). P values < 0.05 were considered statistically significant.

3. Results

3.1. YAP1 expression was decreased in human failing hearts and Dox-induced rat cardiotoxicity model

Many studies revealed that Hippo/YAP1 signal pathway participates in a wide range of biological processes and diseases^{19,22,37,38}. Here, the key genes related to Hippo/YAP1 signal pathway were analyzed by RNAseq analysis of samples from human hearts with dilated cardiomyopathy (Fig. 1A) or from NRCMs with Dox (1 $\mu\text{mol/L}$, 12 h) stimulation (Fig. 1B). The

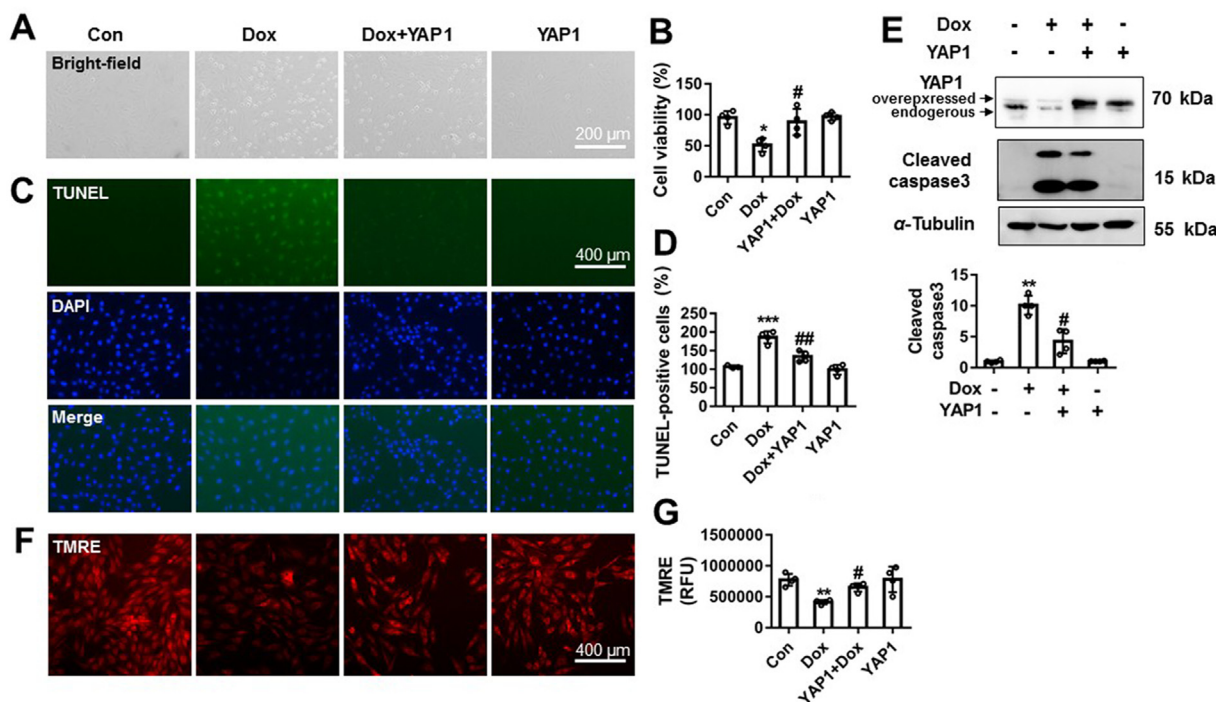


Figure 2 YAP1 protected against Dox-induced cardiomyocytes apoptosis. *Yap1* was overexpressed by using recombinant adenovirus following Dox (1 $\mu\text{mol/L}$, 12 h) stimulation in NRCMs. The morphology of NRCMs was observed by EVOS FL Auto and scale bar was 200 μm (A). The change of cell viability was measured by CCK-8 (B). The TUNEL staining positive NRCMs and nuclear condensation were assayed and scale bar was 400 μm (C). TUNEL-positive cells were quantified and analyzed from four different views (D). The protein change of cleaved caspase 3 was measured by Western blot (E). The changes of mitochondrial membrane potential were detected by TMRE staining (F) and quantified (G). Data were expressed as mean \pm SEM, $n = 4$. * $P < 0.05$, ** $P < 0.01$ vs. control group; # $P < 0.05$, ## $P < 0.01$ vs. Dox group. YAP1, Yes-associated protein 1; Dox, doxorubicin; TUNEL, TdT-mediated dUTP nick end labeling; TMRE, tetramethylrhodamine ethyl ester perchlorate; CCK-8, cell counting kit-8.

transcription of *YAP1* was significantly decreased both in the human cardiomyopathy samples and in Dox-treated NRCMs samples (Fig. 1A and B). Subsequently, we further confirmed the changes of YAP1 by qRT-PCR, Western blot and IF assay. As shown in Fig. 1C, the mRNA level of *YAP1* was decreased in the human failing heart tissue. Similarly, the mRNA level of *Yap1* was significantly decreased in Dox-induced *in vivo* and *in vitro* cardiotoxic model (Fig. 1D and E). The protein expression of YAP1 was also reduced after Dox stimulation at different time point in NRCMs (Fig. 1F). YAP1 is a transcriptional co-activator to regulate the expression of anti-apoptosis genes including *CTGF*³⁹ and *AREG*⁴⁰. Therefore, we measured the changes of YAP1 protein in the nucleic and cytoplasmic fraction of NRCMs and the mRNA levels of its target genes. Dox significantly decreased the expression of YAP1 both in the nucleic and cytoplasmic fraction (Fig. 1G and H) and YAP1 target genes' expression (*Ctgf* and *Areg*, Fig. 1I). These results indicate an association between YAP1 and cardiomyopathy.

3.2. YAP1 relieved Dox-induced cardiomyocytes apoptosis

The significant effects of Dox on the expression of YAP1 encouraged us to explore whether YAP1 was involved in Dox-induced cardiotoxicity. NRCMs were infected with *Yap1* adenovirus for overexpression (2^6 PFU, 48 h). Thirty-six hours later, cardiomyocytes were treated with Dox (1 $\mu\text{mol/L}$) for 12 h. Representative images from bright-field and CCK8 results show that *Yap1* overexpression effectively suppressed Dox-induced

cardiomyocyte death (Fig. 2A and B). *Yap1* overexpression significantly suppressed Dox-induced nuclear condensation and TUNEL positive staining cells (Fig. 2C and D). YAP1 also reduced the cleavage of caspase3 following Dox stimulation (Fig. 2E). Additionally, results from TMRE staining show that *Yap1* overexpression largely suppressed Dox-induced depolarization of mitochondrial membrane (Fig. 2F and G). Furthermore, the expression of *Yap1* in NRCMs was knocked out by targeting sgRNA (Supporting Information Fig. S1A). *Yap1* knockout alone obviously induced cardiomyocyte death (Fig. S1B and S1C). *Yap1* knockout also significantly increased TUNEL positive cardiomyocytes (Fig. S1D) and the expression of cleaved caspase3 (Fig. S1E). TMRE staining results also show that *Yap1* knockout also significantly decreased mitochondrial membrane potential level of NRCMs (Fig. S1F). All these results indicate that *Yap1* overexpression effectively protected against Dox-induced cardiomyocyte apoptosis *in vitro*.

3.3. YAP1 protected against Dox-induced cardiomyocytes apoptosis through TEAD1

As a transcriptional co-activator, YAP1 interacts with TEAD1 (a transcription factor), which is the main downstream target of YAP1, to induce target genes' expression to anti-apoptosis^{18,41}. Here, we explored whether the protective effects of YAP1 against Dox-induced cardiomyocyte apoptosis were mediated by TEAD1. In NRCMs, *Tead1* was silenced by siRNA and the third one was chosen for the following experiments (Fig. 3A). NRCMs were

transfected with silencing RNA targeting *Tead1*, with Ad-*Yap1* co-infection and Dox co-treatment. Overexpression of *Yap1* protected against Dox-caused reduction in cell viability, while *Tead1* silencing effectively abrogated this cardioprotective effects (Fig. 3B). Knockdown of *Tead1* attenuated the inhibitory effects of YAP1 on Dox-induced cardiomyocyte apoptosis, as shown by increased the cleavage of caspase 3, TUNEL positive cell and nuclear condensation (Fig. 3C–E and Supporting Information Fig. S2A). The mitochondrial membrane potential improvement by YAP1 was also significantly decreased by *Tead1* silencing in Dox-treated NRCMs (Fig. 3F and Fig. S2B). These results suggest that the protective effect of YAP1 on Dox-induced cardiomyocytes injury was dependent on TEAD1.

3.4. Isor alleviated Dox-induced cardiomyocytes apoptosis in NRCMs

Isor is a new resveratrol analog (Supporting Information Fig. S3A)²⁷, but with favorable pharmacokinetic profiles superior to resveratrol^{25,26}. Resveratrol was widely studied in cardiovascular diseases including Dox-induced cardiomyopathy^{10,42,43}. Here, we hypothesized that Isor might alleviate Dox-induced cardiomyocytes apoptosis. The effects of Isor on the cell viability were assayed by CCK8, and the result showed that Isor did not influence cell viability even at higher concentration (100 $\mu\text{mol/L}$, Fig. S3B). NRCMs were pre-incubated with Isor at different concentrations (1–40 $\mu\text{mol/L}$) for 1 h

followed by Dox (1 $\mu\text{mol/L}$) stimulation for 12 h. Isor significantly alleviated Dox-induced cardiomyocyte death, as observed from representative images from bright-field (Fig. 4A and Fig. S3C). Cell viability result showed that Isor effectively suppressed Dox-induced cardiotoxicity in a dose-dependent manner (Fig. 4B and Fig. S3D). Isor (2.5–40 $\mu\text{mol/L}$) significantly alleviated Dox-induced TUNEL positive staining cell and nuclear condensation (Fig. 4C and Fig. S3E). Dox-induced cleavage of caspase 3 was also inhibited following Isor treatment (Fig. 4D and Fig. S3F). In addition, Isor obviously blocked Dox-induced decrease in mitochondrial membrane potential (Fig. 4E and Fig. S3G). However, Isor at concentration 1 $\mu\text{mol/L}$ did not show obvious protective effects against Dox-induced cardiotoxicity. Taken together, our results indicate that Isor at the concentrations from 2.5 to 40 $\mu\text{mol/L}$ effectively suppressed Dox-induced cardiomyocyte apoptosis *in vitro*.

3.5. Isor relieved Dox-caused inhibition of YAP1 expression in NRCMs

Given *Yap1* overexpression protected against Dox-induced cardiomyocytes apoptosis through TEAD1 (Figs. 2 and 3), we asked whether the protective effects of Isor on Dox-induced cardiotoxicity through regulating YAP1 expression. NRCMs were pre-incubated with different concentrations of Isor (1–10 $\mu\text{mol/L}$) followed by Dox stimulation for 12 h. As

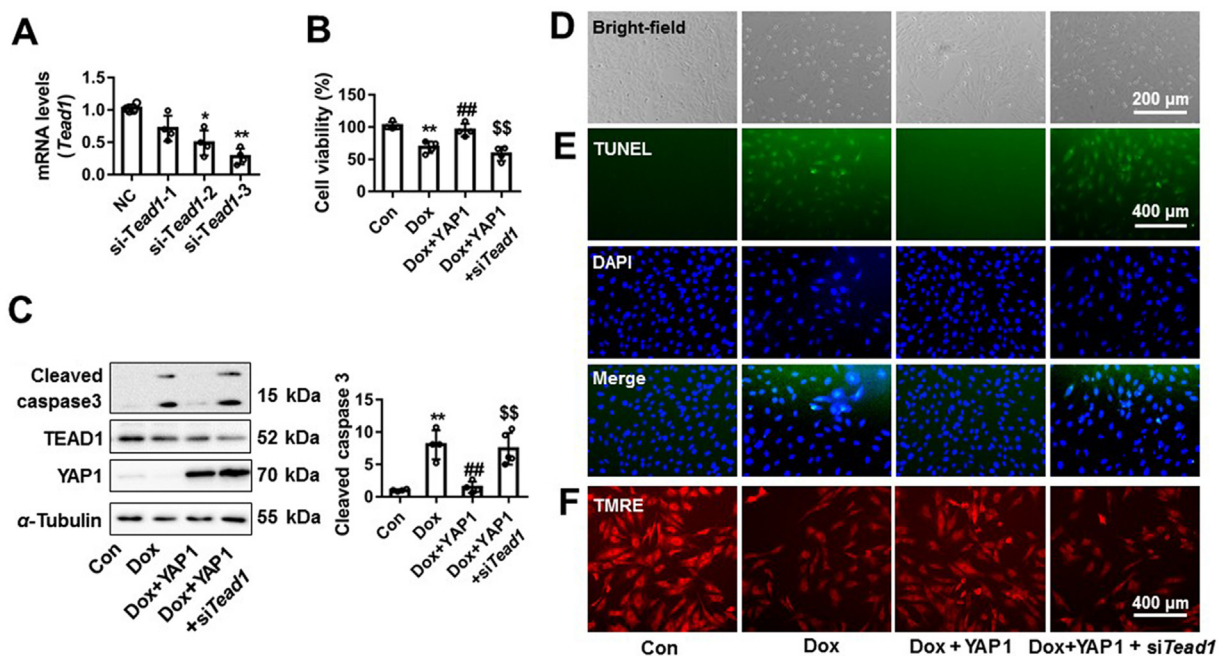


Figure 3 YAP1 protected against Dox-induced cardiomyocytes apoptosis through TEAD1. The silent efficiency of siRNA to *Tead1* was confirmed by qRT-PCR (A). The cell viability change of NRCMs was assayed by CCK-8 (B). The protein changes of cleaved caspase 3, TEAD1 and YAP1 were measured by Western blot (C). The morphology of NRCMs was observed by EVOS FL Auto and scale bar was 200 μm (D). NRCMs were stained by TUNEL and DAPI. TUNEL positive cells and nuclear condensation were observed by EVOS FL Auto, and scale bar was 400 μm (E). The change of mitochondrial membrane potential was measured by TMRE staining (F). Data were expressed as mean \pm SEM, $n = 4$; * $P < 0.05$, ** $P < 0.01$ vs. control group; ## $P < 0.01$ vs. Dox group; \$\$ $P < 0.01$ vs. Dox+YAP1 group. CCK8, cell counting kit-8; TEAD1, TEA domain transcription factor proteins 1; TUNEL, TdT-mediated dUTP nick end labeling; TMRE, tetramethylrhodamine ethyl ester perchlorate; DAPI, 4',6-diamidino-2-phenylindole; YAP1, Yes-associated protein 1.

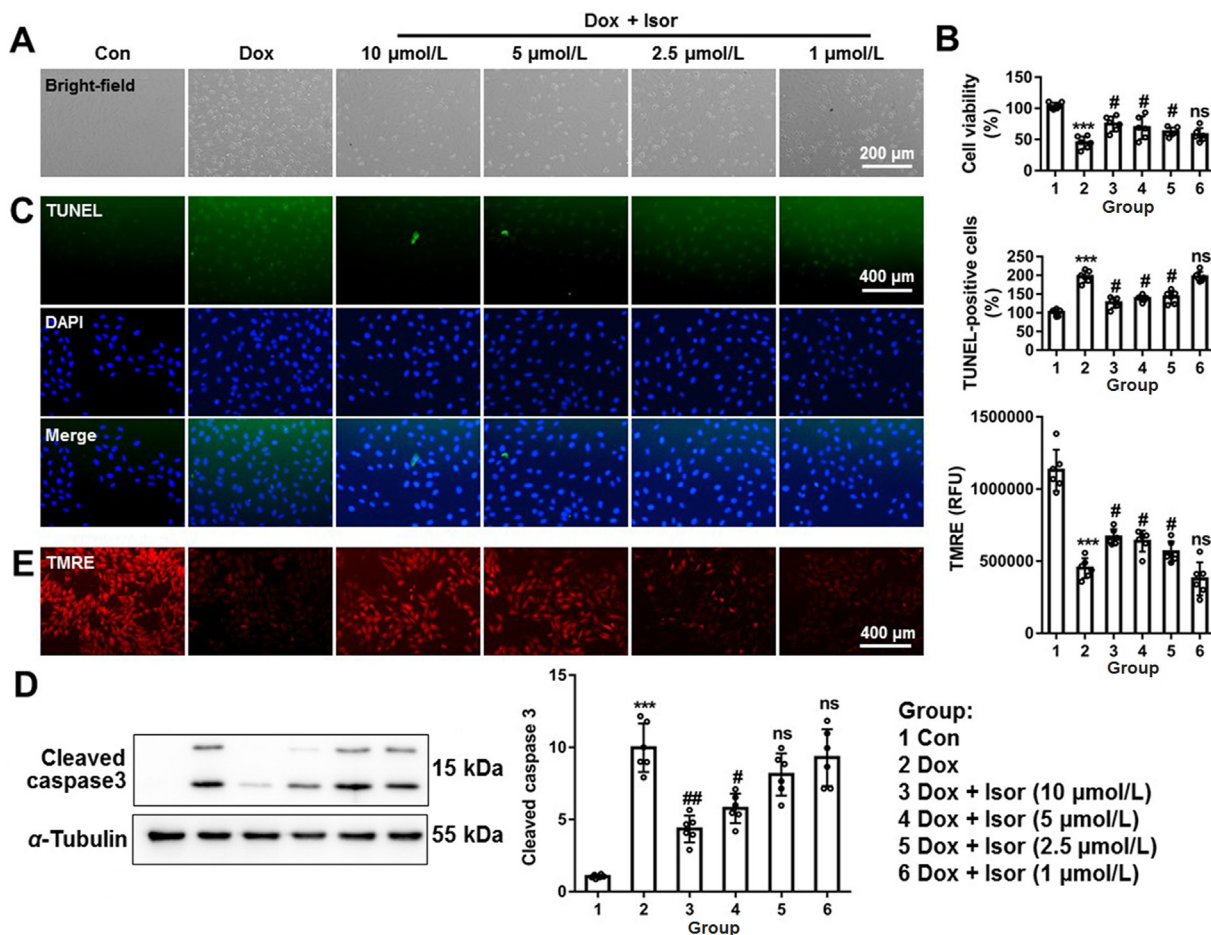


Figure 4 The effects of isorhapontigenin (Isor, 1–10 $\mu\text{mol/L}$) on Dox-induced cardiomyocytes injury. Cardiomyocytes were pre-incubated different concentrations (10, 5, 2.5 and 1 $\mu\text{mol/L}$) of Isor for 1 h and co-treated with Dox (1 $\mu\text{mol/L}$) for 12 h. The cell morphology was observed by EVOS FL Auto and scale bar was 200 μm (A). Cell viability was assayed by CCK-8 (B). Representative graphs of nuclear condensation and TUNEL-staining positive cell were measured by IF and analyzed (C). The protein changes of cleaved caspase 3 were assayed by Western blot (D). Changes of mitochondrial membrane potential were assayed by TMRE staining (E). Data were expressed as mean \pm SEM, $n = 6$; *** $P < 0.001$ vs. control group; # $P < 0.05$, ## $P < 0.01$ vs. Dox group; ns means no significant differences vs. Dox group. CCK-8, cell counting kit-8; IF, immunofluorescence; TMRE, tetramethylrhodamine ethyl ester perchlorate.

shown in Fig. 5A and B, Dox-caused inhibition of *Yap1* mRNA and protein expressions were significantly relieved by Isor at concentrations from 2.5 to 10 $\mu\text{mol/L}$ in a dose dependent manner. By IF staining, Isor (10 $\mu\text{mol/L}$) increased the sub-cellular YAP1 protein located in the cytoplasm and nuclei of Dox-treated NRCMs (Fig. 5C). Compared to Dox group, Western blot results also show that YAP1 protein levels both in the cytoplasmic and nucleic fraction were significantly increased in Isor (10 $\mu\text{mol/L}$) + Dox group (Fig. 5D). The decrease in mRNA expression of *Ctgf* and *Areg* (target genes of YAP1) were also increased by Isor in Dox-treatment NRCMs (Fig. 5E and F).

3.6. YAP1 was involved in the protection of Isor against Dox-induced cardiomyocytes apoptosis

Our results indicate that Isor increased the expression of YAP1 in Dox-treated NRCMs (Fig. 5). Here, we further examined whether YAP1 was involved in the protective effects of Isor against Dox-induced cardiomyocytes apoptosis. *Yap1* was knocked out by targeting sgRNA in NRCMs followed by Isor and Dox co-

treatment. The protective effects of Isor against Dox-induced cardiotoxic effects were effectively blocked by *Yap1* knockout, as indicated by increased cell death (Fig. 6A and B), nuclear condensation, TUNEL positive staining cells (Fig. 6C and Supporting Information Fig. S4A) and the protein expression of cleavage of caspase3 (Fig. 6D). Improved mitochondrial membrane potential by Isor was also destroyed by YAP1 knockout (Fig. 6E and Fig. S4B).

Dobutamine (Dob), a small-molecular regulator of YAP1, promotes the phosphorylation of YAP1 at Ser127, blocks its nuclear translocation and increases the degradation YAP1⁴⁴. To further validate the involvement of YAP1 in the protection of Isor, Dob (10 $\mu\text{mol/L}$) was used in combination with Isor following Dox stimulation. Consistently, Dob blocked the protective effects of Isor on Dox-induced cardiotoxic responses including increase in cell death, nuclear condensation, TUNEL positive staining cells, cleavage of caspase3 and decrease in mitochondrial membrane potential (Fig. 6F–I, Fig. S4D and S4E).

All these results indicate the involvement of YAP1 in the protective effects of Isor on Dox-induced cardiotoxicity *in vitro*.

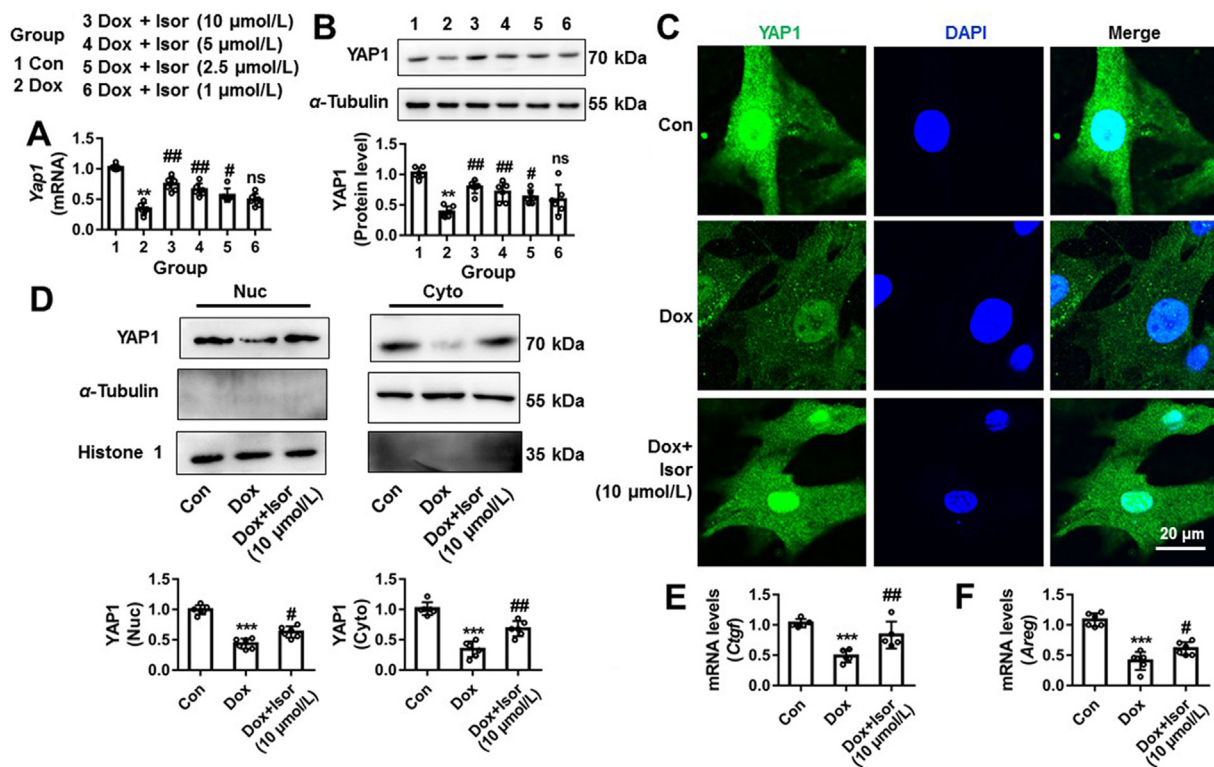


Figure 5 Isorhapontigenin (Isor) relieved Dox-caused inhibition of YAP1 expression in NRCMs. NRCMs were pre-incubated with different concentrations of Isor (10, 5, 2.5 and 1 $\mu\text{mol/L}$) for 1 h followed by Dox stimulation for 12 h. The mRNA expression of *Yap1* was measured by qRT-PCR (A). The protein expression of YAP1 was measured by Western blot (B). IF assay was used to detect the protein changes of YAP1 in NRCMs following Isor (10 $\mu\text{mol/L}$) and Dox (1 $\mu\text{mol/L}$) co-treatment for 12 h (C). Scale bar = 20 μm . Western blot results show the change of YAP1 protein in nucleic and cytoplasmic fraction of NRCMs following Isor (10 $\mu\text{mol/L}$) and Dox (1 $\mu\text{mol/L}$) co-treatment for 12 h (D). The mRNA changes of *Ctgf* (E) and *Areg* (F) were measured by qRT-PCR. Data were expressed as mean \pm SEM, $n = 6$; $**P < 0.01$, $***P < 0.001$ vs. control group; $*P < 0.05$, $##P < 0.01$ vs. Dox group; ns means no significant differences vs. Dox group. Dox, doxorubicin; NRCMs, neonatal rat cardiomyocytes; qRT-PCR, quantitative real-time polymerase chain reaction; CTGF, connective tissue growth factor; AREG, amphiregulin; YAP1, Yes-associated protein 1.

3.7. Isor improved Dox-induced cardiac dysfunction in vivo

Given the effective role of Isor in protecting against Dox-induced cardiotoxicity in NRCMs, we further confirmed the protective effects in C57BL/6 mice. Isor (30 mg/kg/day) was intraperitoneally pre-administrated to mice for 1 week and then Dox was intraperitoneally co-administrated to mice for a cumulative dose of 24 mg/kg (three equal dosages, on the 1st, 6th and 11th day) for 15 days. Control group was treated with vehicle in the same volume solvent.

The gross heart morphometric results showed that the hearts of Dox-treated mice were smaller than control group (Fig. 7A). The inflammatory cell infiltration of Dox group was also shown by HE staining (Fig. 7B and C). Compared to Dox group, Isor could attenuate these effects (Fig. 7A–C). Compared to the Dox group, Isor also increased the size of cardiomyocytes as indicated by WGA staining results (Fig. 7D and Supporting Information Fig. S5A). The heart weight to the body weight (HW/BW) ratio was decreased in the Dox group, which was significantly blocked by Isor treatment (Fig. 7E). Besides, echocardiographic results (Fig. 7F and Supporting Information Table S2) show that treatment with Isor for 3 weeks significantly improved CO, EF and FS in Dox-stimulated mice (Fig. 7G). Decreasing in left ventricular end-systolic anterior wall thickness (LVAW;s, Fig. 7H), left

ventricular end-diastolic anterior wall thickness (LVAW;d, Fig. 7I), left ventricular end-systolic posterior wall thickness (LVPW;s, Fig. 7J) and left ventricular end-diastolic posterior wall thickness (LVPW;d, Fig. 7K) were also increased following Isor treatment in Dox-stimulated mice. Additionally, Dox-induced increase in ventricular end-systolic internal diameter (LVID;s, Fig. S5B) and left ventricular end-diastolic internal diameter (LVID;d, Fig. S5C) were slightly relieved with Isor treatment. Altogether, these results indicate the effectively protective effects of Isor against Dox-induced cardiomyopathy in mice.

3.8. The protective effects of Isor on Dox-induced cardiomyocytes apoptosis and decreased YAP1 expression in vivo

As previously reported, Dox could result in cardiomyocytes apoptosis^{1–4}. We further evaluated the *in vivo* effects of Isor on Dox-induced cardiotoxicity. Our results show that Dox obviously increased TUNEL staining positive staining cells (Fig. 8A and Fig. S5D) and cleavage of caspase3 (Fig. 8B), while Isor treatment significantly blocked these responses. Furthermore, Dox-caused decrease in protein and mRNA levels of YAP1 was significantly reversed by Isor, as indicated by IHC staining (Fig. 8C and Fig. S5E), Western blot (Fig. 8D) and qRT-PCR assay (Fig. 8E). The target gene expressions of YAP1 were also decreased *in vivo*

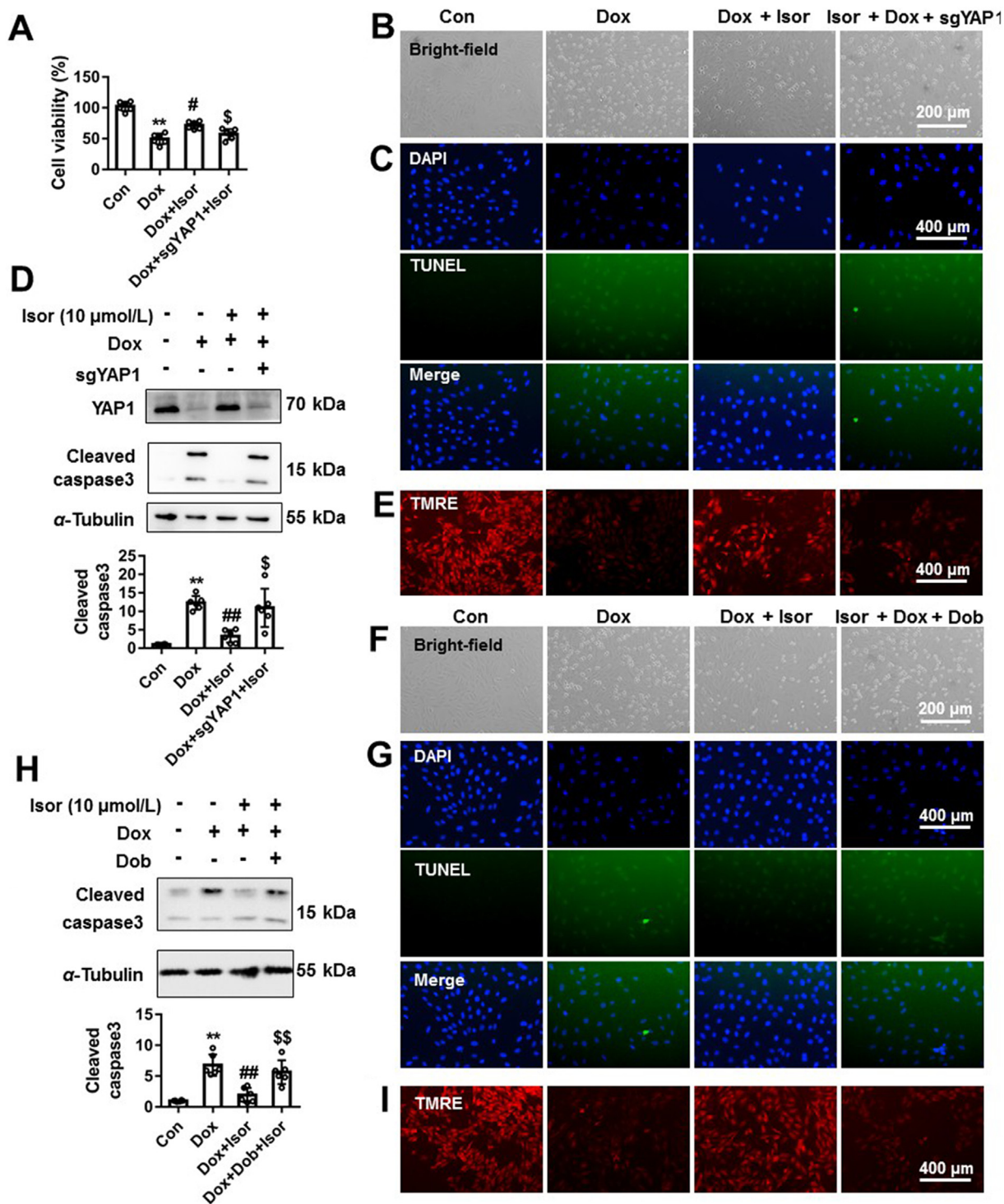


Figure 6 YAP1 was involved in the protection of isorhapontigenin (Isor) on Dox-induced cardiotoxic effects. NRCMs were transfected with sgRNA targeting *Yap1* or treated with YAP1 inhibitor Dob (10 $\mu\text{mol/L}$) before Dox (1 $\mu\text{mol/L}$) and Isor (10 $\mu\text{mol/L}$) co-treatment. Cell viability was measured by CCK-8 (A). The cell morphology was observed by light microscopy, and scale bar was 200 μm (B) and (F). The nuclear condensation and TUNEL positive staining cells were observed and scale bar was 400 μm (C) and (G). The protein change of cleaved caspase 3 was measured by Western blot (D) and (H). The mitochondrial membrane potential changes of NRCMs were detected by TMRE staining, and scale bar was 400 μm (E) and (I). Data were expressed as mean \pm SEM, $n = 6$; ** $P < 0.01$ vs. control group; # $P < 0.05$, ## $P < 0.01$ vs. Dox group; \$ $P < 0.05$, \$\$ $P < 0.01$ vs. Dox+Isor group. Isor, isorhapontigenin; Dox, doxorubicin; NRCMs, neonatal rat cardiomyocytes; Dob, dobutamine; TMRE, tetramethylrhodamine ethyl ester perchlorate; YAP1, Yes-associated protein 1.

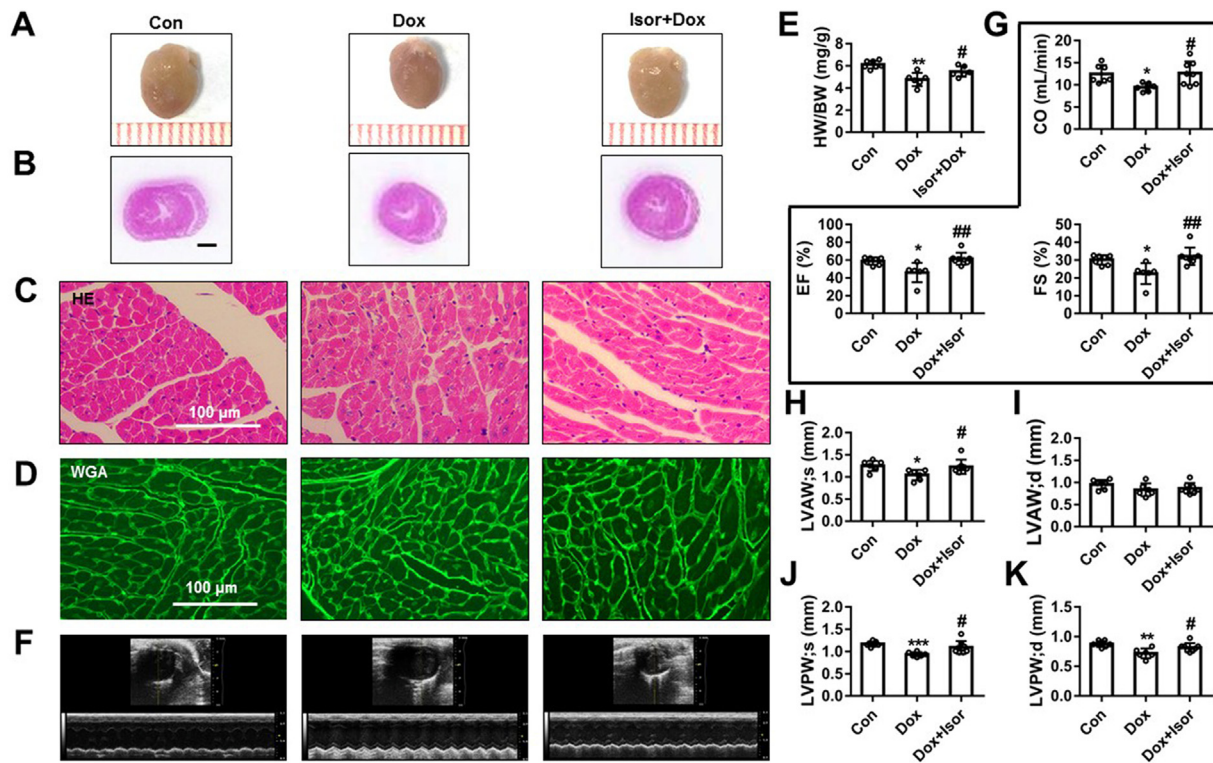


Figure 7 Isor improved Dox-induced cardiac dysfunction *in vivo*. C57BL/6 mice were pre-treated with Isor (30 mg/kg/day) for 1 week followed with Dox stimulation for 2 weeks. The gross hearts from mice were shown (A). The hematoxylin–eosin (HE) staining of heart tissues was shown, and scale bar was 100 μ m (B) and (C). Wheat germ agglutinin (WGA) staining of heart tissues was shown, and scale bar was 100 μ m (D). Heart weight to body weight ratio (HW/BW) was shown (E), $n = 7$ in control group, $n = 6$ in Dox group and Dox+Isor group. Representative echocardiographic graphs are shown (F). The echocardiographic parameters were measured, including cardiac output (CO), ejection fraction (EF), fractional shortening (FS) (G), left ventricular anterior wall thickness (LVAW) at systolic end-stage and diastolic end-stage (H) and (I) and left ventricular posterior wall thickness (LVPW) at systolic end-stage and diastolic end-stage (J) and (K), $n = 7$ in control group, $n = 6$ in Dox group and $n = 8$ in Dox+Isor group. Data were expressed as mean \pm SEM; * $P < 0.05$, ** $P < 0.01$ vs. control group; # $P < 0.05$, ## $P < 0.01$ vs. Dox group. Isor, isorhapontigenin; Dox, doxorubicin.

by Dox, while Isor could partly reverse these changes (Fig. 8F and G). These results suggest that Isor has the protective effect on cardiomyocytes apoptosis and increased YAP1 expression in Dox-induced cardiotoxicity model in mice.

4. Discussion

The clinical application of Dox is limited for its time- and dose-dependent cardiotoxicity, which finally leads to irreversibly cardiomyopathy and heart failure^{2,3,8,45}. Several agents have been identified for anti-Dox-induced cardiomyopathy, such as vitamin E, carvedilol, resveratrol and 7-monoxyethylrutin^{14,46–48}, but these agents are far from satisfaction¹². In this study, YAP1 was identified as a new target for the prevention against Dox-induced cardiotoxicity in a TEAD1-dependent manner. Moreover, Isor attenuated Dox-induced cardiotoxicity by increasing YAP1 expression. By targeting YAP1, Isor may be a new candidate compound to fight against Dox-induced cardiotoxicity.

YAP1, the terminal effector of the Hippo signaling pathway, plays an important role in a broad range of biological functions¹⁷. Hippo–YAP1 pathway has protective effect on the regulation of cardiac development and regeneration of embryonic heart^{19,22,37,38}. In embryonic heart, YAP1 activates insulin-like growth factor, interacts with β -catenin and regulates WNT signaling to restrict cardiomyocyte proliferation and controls

heart size^{18,49–51}. In post-natal heart, cardiac-specific *Yap1* overexpression relieves MI-induced cardiac injury by regulating forkhead box class O1 (FOXO1) or by directly targeting PIK3CB to activate phosphoinositol-3-kinase-AKT pathway^{15,52,53}. To date, the role of Hippo–YAP1 pathway in Dox-induced cardiotoxicity has not been reported. RNAseq analysis of Hippo pathway and the validation results consistently showed that *YAP1* expression was obviously decreased in human failing hearts and Dox-induced cardiotoxicity. *Yap1* overexpression effectively relieved Dox-induced cardiotoxicity as indicated by decreased apoptosis and increased mitochondrial membrane potential.

As a transcription factor, TEAD1 regulates its target genes expression (e.g., *Ctgf* and *Areg*) to fight against cell apoptosis^{18,41,49}, proliferation¹⁸, epithelial mesenchymal transformation (EMT), and oncogenic transformation^{21,24}. YAP1 acts as the transcriptional co-factor of TEAD1, facilitates TEAD1 to regulate target genes expression^{18,41}. Our results indicate that the protective effects of YAP1 on Dox-induced cardiotoxicity.

Resveratrol has been reported to protect from various cardiovascular diseases including cardiac hypertrophy and Dox-induced cardiomyopathy^{10,42,43}. As a resveratrol analog, Isor shows favorable pharmacokinetic profiles superior to that of resveratrol, as indicated by its dose-normalized maximal plasma concentrations ($C_{max}/dose$), dose-normalized plasma exposures (AUC/dose)

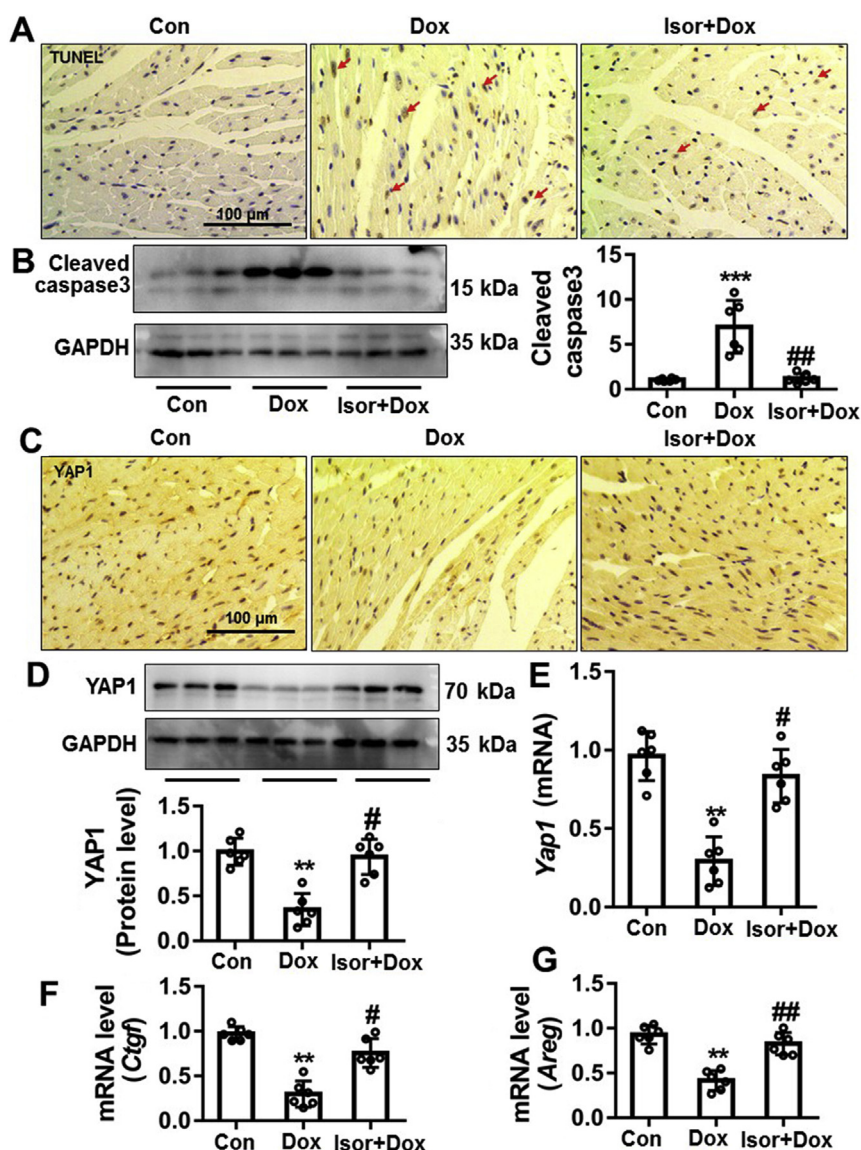


Figure 8 Isor alleviated Dox-induced cardiomyocytes apoptosis and increased YAP1 expression *in vivo*. The heart tissue of mice was stained with TUNEL and observed by EVOS FL Auto. Representative graphs are shown and scale bar is 100 μ m (A). The change of cleaved caspase 3 levels in the heart tissue of mice was measured by Western blot (B). The protein level of YAP1 in the heart of mice was assayed by IHC and scale bar is 100 μ m (C). The protein and mRNA levels of *Yap1* in the heart of mice were measured by Western blot (D) and qRT-PCR (E). The mRNA expressions of YAP1' target genes (*Ctgf* and *Areg*) were assayed by qRT-PCR (F) and (G). Data were expressed as mean \pm SEM, $n = 6$; * $P < 0.05$, ** $P < 0.01$, *** $P < 0.001$ vs. control group; # $P < 0.05$, ## $P < 0.01$ vs. Dox group. YAP1, Yes-associated protein 1; Isor, isorhapontigenin; Dox, doxorubicin; IHC, immunohistochemistry; qRT-PCR, quantitative real-time polymerase chain reaction; CTGF, connective tissue growth factor; AREG, amphiregulin.

and oral bioavailability (F) are approximately 2–3-fold greater than resveratrol^{25,26}. Actually, the protective effects of resveratrol on Dox-induced cardiomyopathy were limited¹⁴. Hence, we wanted to know whether Isor may have more pronounced effects on cardiovascular diseases than resveratrol. Isor could effectively protect against cardiac hypertrophy or myocardial infarction by regulating nuclear factor kappa-B, anti-microbial protein (AP-1)²⁷ or by decreasing ROS and inflammatory responses³⁶. In this study, Isor also showed significant therapeutic effects against Dox-induced cardiotoxicity *in vitro* and *in vivo*.

In the process of playing its biological function and therapeutic effects, Isor involves various signal molecules and related signal transduction pathways^{27–36}. By inhibiting MAPK-

associated pathways, Isor suppresses interleukin-1 β -induced inflammation and cartilage matrix damage in rat chondrocytes³⁰. Compared to resveratrol, Isor binds to P2Y12 receptor (ADP receptor) and inhibits ADP-stimulated platelet activation by decreasing AKT phosphorylation²⁹. Isor inhibits cancer cell growth and induces apoptosis *via* regulating EGFR pathways³⁴ and upregulating miR-137 transcription³³ or increasing the binding of FOXO1 to p27 promoter⁵⁴. Our results show that Isor promoted the transcription of YAP1 in Dox-induced cardiotoxicity model.

The transcription of *Yap1* gene is regulated by a variety of factors^{55–62}. Some miRNAs regulate the expression of *Yap1*, such as miR-4319, miR-506, miR-375 and miR-186^{55–58}. Circular

RNA negatively regulates YAP1 protein levels by suppressing translation initiation machinery⁵⁹. β -Catenin/T-cell factor 4 (TCF4) complexes directly bound to DNA enhancer element to promote *YAP1* expression in colorectal carcinoma cells⁶⁰. *YAP1* expression is strongly correlated to its promoter methylation in breast cancer patients⁶². Besides, we previously discovered that β -catenin pathway was tightly related to Dox-induced cardiotoxicity⁴⁵. Meanwhile, demethylase and the methylation of histone were significantly changed (date not shown). Hence, we speculated that the inhibition of YAP1 expression in Dox-induced cardiotoxicity model might be related to its promoter methylation or β -catenin pathway. But this possibility needs further confirmation.

Based on our work, it could be conclusive that Isor protected against doxorubicin-induced cardiotoxicity via increasing *Yap1* expression. Whether Isor is superior to resveratrol to fight against Dox-induced cardiotoxicity is unclear. The detailed mechanisms of the changes of YAP1 at transcription level after Dox or Isor treatment remains to be further explored.

5. Conclusions

Isor effectively protected against Dox-induced cardiotoxicity and improved cardiac function by increasing the expression of YAP1. It might be crucial to treat with Isor or overexpressed *Yap1* when the occurrence of Dox-induced cardiotoxicity. In light of this, our findings may have immediate implications on the development of a new therapeutic strategy for overcoming Dox-induced cardiotoxicity by targeting Isor–YAP1–TEAD1 axis.

Acknowledgments

This research was supported by grants from the National Natural Science Foundation of China (81872860, 81803521, 81673433), National Major Special Projects for the Creation and Manufacture of New Drugs (2019ZX09301104, China), Local Innovative and Research Teams Project of Guangdong Pearl River Talents Program (2017BT01Y093, China), National Engineering and Technology Research Center for New drug Druggability Evaluation (Seed Program of Guangdong Province, 2017B090903004, China), Natural Science Foundation of Guangdong Province (2019A1515010273, China), Foundation from Guangdong Traditional Medicine Bureau (20191060, China), Fundamental Research Funds for the Central Universities (19ykpy131, China) and Research and Industrialization team of *Taxus chinensis* var. *mairei* (2014YT02S044, China).

Author contributions

Panxia Wang and Minghui Wang designed the experiment, analyzed the data and wrote the manuscript. Yuehuai Hu, Jianxing Chen and Yanjun Cao helped perform the experiments. Zhongkai Wu provided samples from human heart. Juan Shen and Jing Lu designed and revised the manuscript. Peiqing Liu was responsible for supervision.

Conflicts of interest

The authors declare no conflicts of interests.

Appendix A. Supporting information

Supporting data to this article can be found online at <https://doi.org/10.1016/j.apsb.2020.10.017>.

References

1. Gyongyosi M, Lukovic D, Zlabinger K, Spannbaauer A, Gugerell A, Pavo N, et al. Liposomal doxorubicin attenuates cardiotoxicity via induction of interferon-related DNA damage resistance. *Cardiovasc Res* 2019;**116**:970–82.
2. Wang P, Wang L, Lu J, Hu Y, Wang Q, Li Z, et al. SESN2 protects against doxorubicin-induced cardiomyopathy via rescuing mitophagy and improving mitochondrial function. *J Mol Cell Cardiol* 2019;**133**: 125–37.
3. Lu J, Li J, Hu Y, Guo Z, Sun D, Wang P, et al. Chrysophanol protects against doxorubicin-induced cardiotoxicity by suppressing cellular PARylation. *Acta Pharm Sin B* 2019;**9**:782–93.
4. Bartlett JJ, Trivedi PC, Pulinilkunnil T. Autophagic dysregulation in doxorubicin cardiomyopathy. *J Mol Cell Cardiol* 2017;**104**:1–8.
5. Fazio S, Palmieri EA, Ferravante B, Bone F, Biondi B, Sacca L. Doxorubicin-induced cardiomyopathy treated with carvedilol. *Clin Cardiol* 1998;**21**:777–9.
6. Octavia Y, Tocchetti CG, Gabrielson KL, Janssens S, Crijns HJ, Moens AL. Doxorubicin-induced cardiomyopathy: from molecular mechanisms to therapeutic strategies. *J Mol Cell Cardiol* 2012;**52**: 1213–25.
7. Zhang S, Liu X, Bawa-Khalife T, Lu LS, Lyu YL, Liu LF, et al. Identification of the molecular basis of doxorubicin-induced cardiotoxicity. *Nat Med* 2012;**18**:1639–42.
8. Gao S, Li H, Feng XJ, Li M, Liu ZP, Cai Y, et al. α -Enolase plays a catalytically independent role in doxorubicin-induced cardiomyocyte apoptosis and mitochondrial dysfunction. *J Mol Cell Cardiol* 2015;**79**: 92–103.
9. Dhingra R, Guberman M, Rabinovich-Nikitin I, Gerstein J, Margulets V, Gang H, et al. Impaired NF- κ B signalling underlies cyclophilin D-mediated mitochondrial permeability transition pore opening in doxorubicin cardiomyopathy. *Cardiovasc Res* 2019;**116**: 1161–74.
10. Tatlidede E, Schirli O, Velioglu-Ogunc A, Cetinel S, Yegen BC, Yarat A, et al. Resveratrol treatment protects against doxorubicin-induced cardiotoxicity by alleviating oxidative damage. *Free Radic Res* 2009;**43**:195–205.
11. Gu C, Li T, Jiang S, Yang Z, Lv J, Yi W, et al. AMP-activated protein kinase sparks the fire of cardioprotection against myocardial ischemia and cardiac ageing. *Ageing Res Rev* 2018;**47**:168–75.
12. Lv J, Deng C, Jiang S, Ji T, Yang Z, Wang Z, et al. Blossoming 20: the energetic regulator's birthday unveils its versatility in cardiac diseases. *Theranostics* 2019;**9**:466–76.
13. Berthiaume JM, Oliveira PJ, Fariss MW, Wallace KB. Dietary vitamin E decreases doxorubicin-induced oxidative stress without preventing mitochondrial dysfunction. *Cardiovasc Toxicol* 2005;**5**:257–67.
14. Bruynzeel AM, Niessen HW, Bronzwaer JG, van der Hoeven JJ, Berkhof J, Bast A, et al. The effect of monohydroxyethylrutoside on doxorubicin-induced cardiotoxicity in patients treated for metastatic cancer in a phase II study. *Br J Canc* 2007;**97**:1084–9.
15. Lin Z, von Gise A, Zhou P, Gu F, Ma Q, Jiang J, et al. Cardiac-specific YAP activation improves cardiac function and survival in an experimental murine MI model. *Circ Res* 2014;**115**:354–63.
16. Ragni CV, Diguat N, Le Garrec JF, Novotova M, Resende TP, Pop S, et al. Amotl1 mediates sequestration of the Hippo effector Yap1 downstream of Fat4 to restrict heart growth. *Nat Commun* 2017;**8**: 14582.
17. Kodaka M, Hata Y. The mammalian Hippo pathway: regulation and function of YAP1 and TAZ. *Cell Mol Life Sci* 2015;**72**:285–306.
18. von Gise A, Lin Z, Schlegelmilch K, Honor LB, Pan GM, Buck JN, et al. YAP1, the nuclear target of Hippo signaling, stimulates heart

- growth through cardiomyocyte proliferation but not hypertrophy. *Proc Natl Acad Sci U S A* 2012;**109**:2394–9.
19. Wang J, Liu S, Heallen T, Martin JF. The Hippo pathway in the heart: pivotal roles in development, disease, and regeneration. *Nat Rev Cardiol* 2018;**15**:672–84.
 20. Moya IM, Halder G. Hippo-YAP/TAZ signalling in organ regeneration and regenerative medicine. *Nat Rev Mol Cell Biol* 2019;**20**:211–26.
 21. Xiao Y, Hill MC, Zhang M, Martin TJ, Morikawa Y, Wang S, et al. Hippo signaling plays an essential role in cell state transitions during cardiac fibroblast development. *Dev Cell* 2018;**45**:153–69. e156.
 22. Del Re DP, Yang Y, Nakano N, Cho J, Zhai P, Yamamoto T, et al. Yes-associated protein isoform 1 (Yap1) promotes cardiomyocyte survival and growth to protect against myocardial ischemic injury. *J Biol Chem* 2013;**288**:3977–88.
 23. Yang Y, Del Re DP, Nakano N, Sciarretta S, Zhai P, Park J, et al. miR-206 mediates YAP-induced cardiac hypertrophy and survival. *Circ Res* 2015;**117**:891–904.
 24. Xiao Y, Hill MC, Li L, Deshmukh V, Martin TJ, Wang J, et al. Hippo pathway deletion in adult resting cardiac fibroblasts initiates a cell state transition with spontaneous and self-sustaining fibrosis. *Genes Dev* 2019;**33**:1491–505.
 25. Fernandez-Marin MI, Guerrero RF, Garcia-Parrilla MC, Puertas B, Richard T, Rodriguez-Werner MA, et al. Isorhapontigenin: a novel bioactive stilbene from wine grapes. *Food Chem* 2012;**135**:1353–9.
 26. Dai Y, Yeo SCM, Barnes PJ, Donnelly LE, Loo LC, Lin HS. Pre-clinical pharmacokinetic and metabolomic analyses of isorhapontigenin, a dietary resveratrol derivative. *Front Pharmacol* 2018;**9**:753.
 27. Li HL, Wang AB, Huang Y, Liu DP, Wei C, Williams GM, et al. Isorhapontigenin, a new resveratrol analog, attenuates cardiac hypertrophy via blocking signaling transduction pathways. *Free Radic Biol Med* 2005;**38**:243–57.
 28. Yeo SCM, Fenwick PS, Barnes PJ, Lin HS, Donnelly LE. Isorhapontigenin, a bioavailable dietary polyphenol, suppresses airway epithelial cell inflammation through a corticosteroid-independent mechanism. *Br J Pharmacol* 2017;**174**:2043–59.
 29. Ravishankar D, Albadawi DAI, Chaggar V, Patra PH, Williams HF, Salamah M, et al. Isorhapontigenin, a resveratrol analogue selectively inhibits ADP-stimulated platelet activation. *Eur J Pharmacol* 2019;**862**:172627.
 30. Ma Y, Tu C, Liu W, Xiao Y, Wu H. Isorhapontigenin suppresses interleukin-1 β -induced inflammation and cartilage matrix damage in rat chondrocytes. *Inflammation* 2019;**42**:2278–85.
 31. Wang H, Yang YL, Zhang H, Yan H, Wu XJ, Zhang CZ. Administration of the resveratrol analogues isorhapontigenin and heyneanol-A protects mice hematopoietic cells against irradiation injuries. *BioMed Res Int* 2014;**2014**:282657.
 32. Luo Y, Tian Z, Hua X, Huang M, Xu J, Li J, et al. Isorhapontigenin (ISO) inhibits stem cell-like properties and invasion of bladder cancer cell by attenuating CD44 expression. *Cell Mol Life Sci* 2019;**77**:351–63.
 33. Guo X, Huang H, Jin H, Xu J, Risal S, Li J, et al. ISO, via upregulating miR-137 transcription, inhibits GSK3 β –HSP70–MMP-2 axis, resulting in attenuating urothelial cancer invasion. *Mol Ther Nucleic Acids* 2018;**12**:337–49.
 34. Zhu C, Zhu Q, Wu Z, Yin Y, Kang D, Lu S, et al. Isorhapontigenin induced cell growth inhibition and apoptosis by targeting EGFR-related pathways in prostate cancer. *J Cell Physiol* 2018;**233**:1104–19.
 35. Liang Y, Zhu J, Huang H, Xiang D, Li Y, Zhang D, et al. SESN2/sestrin 2 induction-mediated autophagy and inhibitory effect of isorhapontigenin (ISO) on human bladder cancers. *Autophagy* 2016;**12**:1229–39.
 36. Abbas AM. Cardioprotective effect of resveratrol analogue isorhapontigenin versus omega-3 fatty acids in isoproterenol-induced myocardial infarction in rats. *J Physiol Biochem* 2016;**72**:469–84.
 37. Zhao WB, Lu Q, Nguyen MN, Su Y, Ziemann M, Wang LN, et al. Stimulation of beta-adrenoceptors up-regulates cardiac expression of galectin-3 and BIM through the Hippo signalling pathway. *Br J Pharmacol* 2019;**176**:2465–81.
 38. Yu W, Ma X, Xu J, Heumuller AW, Fei Z, Feng X, et al. VGLL4 plays a critical role in heart valve development and homeostasis. *PLoS Genet* 2019;**15**:e1007977.
 39. Martini A, Marioni G, Zanoletti E, Cappellesso R, Stramare R, Fasanaro E, et al. YAP, TAZ and AREG expression in eighth cranial nerve schwannoma. *Int J Biol Markers* 2017;**32**:e319–24.
 40. Ahn EY, Kim JS, Kim GJ, Park YN. RASSF1A-mediated regulation of AREG via the Hippo pathway in hepatocellular carcinoma. *Mol Canc Res* 2013;**11**:748–58.
 41. Zhou Y, Huang T, Cheng AS, Yu J, Kang W, To KF. The TEAD family and its oncogenic role in promoting tumorigenesis. *Int J Mol Sci* 2016;**17**:138.
 42. Cappetta D, Esposito G, Piegari E, Russo R, Ciuffreda LP, Rivellino A, et al. SIRT1 activation attenuates diastolic dysfunction by reducing cardiac fibrosis in a model of anthracycline cardiomyopathy. *Int J Cardiol* 2016;**205**:99–110.
 43. Deus CM, Zehowski C, Nordgren K, Wallace KB, Skildum A, Oliveira PJ. Stimulating basal mitochondrial respiration decreases doxorubicin apoptotic signaling in H9c2 cardiomyoblasts. *Toxicology* 2015;**334**:1–11.
 44. Fujii M. Exploration of a new drug that targets YAP. *J Biochem* 2012;**152**:209–11.
 45. Hu Y, Guo Z, Lu J, Wang P, Sun S, Zhang Y, et al. sFRP1 has a biphasic effect on doxorubicin-induced cardiotoxicity in a cellular location-dependent manner in NRCMs and Rats. *Arch Toxicol* 2019;**93**:533–46.
 46. Hadi N, Yousif NG, Al-amran FG, Huntei NK, Mohammad BI, Ali SJ. Vitamin E and telmisartan attenuates doxorubicin induced cardiac injury in rat through down regulation of inflammatory response. *BMC Cardiovasc Disord* 2012;**12**:63.
 47. Abuosa AM, Elsheikh AH, Qureshi K, Abrar MB, Kholeif MA, Kinsara AJ, et al. Prophylactic use of carvedilol to prevent ventricular dysfunction in patients with cancer treated with doxorubicin. *Indian Heart J* 2018;**70 Suppl 3**:s96–100.
 48. Abe J, Yamada Y, Takeda A, Harashima H. Cardiac progenitor cells activated by mitochondrial delivery of resveratrol enhance the survival of a doxorubicin-induced cardiomyopathy mouse model via the mitochondrial activation of a damaged myocardium. *J Control Release* 2018;**269**:177–88.
 49. Heallen T, Zhang M, Wang J, Bonilla-Claudio M, Klysik E, Johnson RL, et al. Hippo pathway inhibits Wnt signaling to restrain cardiomyocyte proliferation and heart size. *Science* 2011;**332**:458–61.
 50. Xin M, Kim Y, Sutherland LB, Murakami M, Qi X, McAnally J, et al. Hippo pathway effector Yap promotes cardiac regeneration. *Proc Natl Acad Sci U S A* 2013;**110**:13839–44.
 51. Xin M, Kim Y, Sutherland LB, Qi X, McAnally J, Schwartz RJ, et al. Regulation of insulin-like growth factor signaling by Yap governs cardiomyocyte proliferation and embryonic heart size. *Sci Signal* 2011;**4**:ra70.
 52. Shao D, Zhai P, Del Re DP, Sciarretta S, Yabuta N, Nojima H, et al. A functional interaction between Hippo-YAP signalling and FoxO1 mediates the oxidative stress response. *Nat Commun* 2014;**5**:3315.
 53. Lin Z, Zhou P, von Gise A, Gu F, Ma Q, Chen J, et al. *Pi3kcb* links Hippo-YAP and PI3K-AKT signaling pathways to promote cardiomyocyte proliferation and survival. *Circ Res* 2015;**116**:35–45.
 54. Jiang G, Huang C, Li J, Huang H, Wang J, Li Y, et al. Transcriptional and post-transcriptional upregulation of p27 mediates growth inhibition of isorhapontigenin (ISO) on human bladder cancer cells. *Carcinogenesis* 2018;**39**:482–92.
 55. Ruan T, He X, Yu J, Hang Z. MicroRNA-186 targets Yes-associated protein 1 to inhibit Hippo signaling and tumorigenesis in hepatocellular carcinoma. *Oncol Lett* 2016;**11**:2941–5.
 56. Zhang ZW, Men T, Feng RC, Li YC, Zhou D, Teng CB. miR-375 inhibits proliferation of mouse pancreatic progenitor cells by targeting YAP1. *Cell Physiol Biochem* 2013;**32**:1808–17.

57. Wang Y, Cui M, Sun BD, Liu FB, Zhang XD, Ye LH. MiR-506 suppresses proliferation of hepatoma cells through targeting YAP mRNA 3'UTR. *Acta Pharmacol Sin* 2014;**35**:1207–14.
58. Yang Y, Li H, Liu Y, Chi C, Ni J, Lin X. MiR-4319 hinders YAP expression to restrain non-small cell lung cancer growth through regulation of LIN28-mediated RFX5 stability. *Biomed Pharmacother* 2019;**115**:108956.
59. Wu N, Yuan Z, Du KY, Fang L, Lyu J, Zhang C, et al. Translation of yes-associated protein (YAP) was antagonized by its circular RNA via suppressing the assembly of the translation initiation machinery. *Cell Death Differ* 2019;**26**:2758–73.
60. Konsavage Jr WM, Kyler SL, Rennoll SA, Jin G, Yochum GS. Wnt/ β -catenin signaling regulates Yes-associated protein (YAP) gene expression in colorectal carcinoma cells. *J Biol Chem* 2012;**287**:11730–9.
61. Xia W, Su L, Jiao J. Cold-induced protein RBM3 orchestrates neurogenesis via modulating Yap mRNA stability in cold stress. *J Cell Biol* 2018;**217**:3464–79.
62. Real SAS, Parveen F, Rehman AU, Khan MA, Deo SVS, Shukla NK, et al. Aberrant promoter methylation of YAP gene and its subsequent downregulation in Indian breast cancer patients. *BMC Canc* 2018;**18**:711.